Numerical Evaluation of Low-Dimensional Energy Spectrum and Carrier Statistics for Nanostructure Device Application

Ismail Saad[1], Khairul Anuar Mohamad[1], Nurmin Bolong[1], Abu Bakar Abd Rahman[1] and Vijay K. Arora[2]

[1]Nano Engineering & Materials (NEMs) Research Group, School of Engineering & IT, Universiti Malaysia Sabah, 88999, Kota Kinabalu, Sabah
[2]Division of Engineering and Physics, Wilkes University, Wilkes-Barre, PA 18766, U. S. A.
ismail_s@ums.edu.my / ismailsaad07@gmail.com

***Abstract*— Numerical evaluation of energy spectrum and carrier statistics for nanostructure device application is presented. The low-dimensional energy spectrum was successfully derived for the respective quasi 3D, 2D and 1D system that invoked the effect of quantum confinement (QCE) comparable to the De Broglie wavelength ($\lambda_D \cong 10nm$). For non-degenerately (ND) doped samples the Fermi-Dirac (FD) integral is well approximated by Boltzmann statistics. However, in degenerate doped quasi 3D, 2D and 1D device, the FD integral is found to be approximated by order one-half, zero and minus one-half respectively. The Fermi energy is revealed to be a weak (logarithmic) function of carrier concentration, but varies linearly with temperature in the ND regime. However, for strongly degenerate statistics, the Fermi energy is independent of temperature and is a strong function of carrier concentration.**

Keywords - Energy spectrum, carrier statistics, nano-MOSFET, De Broglie wavelength, quantum confinement effect (QCE), nanowire

I. Introduction

As devices are being scaled down in decananometer regime, the physics-based analytical interpretation of carrier statistics in a low-dimensional nanostructure device is essentially needed [1-3]. The quantum confinement effect (QCE) and ballistic (B) carrier transport in nano-devices has been heavily investigated and modeled to spur proper understanding of insight of the nano-electronics circuits [4-9]. The numerical analysis of carrier statistics that invoked QCE and B phenomenon of a nanostructure device is elaborated in this paper. The appropriate approximation of Boltzmann and Fermi-Dirac statistics applied to non-degenerate (ND) and degenerate (D) regime for all dimensionality was employed and explained intuitively.

The fundamental physics of quantum confinement effect (QCE) is presented in section II. Energy spectrum analysis in the low-dimensional system for quasi 3D, 2D and 1D is presented in section III. The computation of carrier statistics that leads to proper approximation in all degeneracy level is elucidated in section IV. Section V gives the results and analysis of carrier statistics in all dimensions of degeneracy and its dependency on carrier concentrations. The major findings of this work are summarized in the concluding Section VI.

II. Quantum Confinement Effect

The channel in a nano-scale MOSFET is indeed a quantum one that is constrained by the gate electric field forming an approximately linear quantum well. Contrary to many researchers, no heating of the electrons by the gate is possible. Rather the gate confines the electron to length z_{QM} comparable to the de Broglie wavelength. The energy spectrum is digital (quantum) in the z-direction perpendicular to the gate while other two cartesian directions with lengths L_x and L_y are analog (or classical). This confinement makes the channel quasi two dimensional (QTD) [10-12]:

$$\varepsilon_{ki} = \frac{\hbar^2 k_x^2}{2m_1^*} + \frac{\hbar^2 k_y^2}{2m_2^*} + \varepsilon_i \tag{1}$$

with

$$\varepsilon_i = \xi_i E_o \approx \left[\frac{\hbar^2}{2m_3}\right]^{\frac{1}{3}} \left[\frac{3\pi q}{2} E_t \left(i + \frac{3}{4}\right)\right]^{\frac{2}{3}} \qquad i=0,1,2,3.. \tag{2}$$

$$E_o = \left(\frac{\hbar^2 q^2 E_t^2}{2m_3^*}\right)^{1/3} \tag{3}$$

where $k_{x,y}$ are the momentum vectors in the analog two-dimensional x-y plane and ε_i is the quantized energy in the digitized z-direction. $m^*_{1,2}$ is the effective mass in the x-y plane of the QTD channel and m^*_3 is the effective mass in z-direction for a given conduction valley. ξ_i are the zeros of the Airy function ($Ai(-\xi_i)=0$) with ξ_0=2.33811, ξ_1=4.08795 and ξ_2=5.52056. For (100) Si MOSFET, the conduction band energy surfaces are six ellipsoids with longitudinal direction along ± *x,y,z* in k-space [13]. The two valleys have $m^*_3 = m_\ell$ =0.916 m_o and four valleys with $m^*_3 = m_t$ =0.19 m_o. $\varepsilon_o = \xi_0 E_o$ is the ground state energy corresponding to i=0 with m_3 = 0.916 m_o for the two valleys. Other four valleys are not occupied in the quantum limit when all electrons are in the lowest energy state. $m^*_{1,2}$ =0.19m_o is the conductivity effective mass in the x-y plane of the QTD channel for lower two valleys. E_t is the electric field generated by the gate, which in the strong inversion regime.

$$E_t \approx \frac{V_{GT} + V_T}{6t_{ox}} \tag{4}$$

Here $V_{GT} = V_{GS} - V_T$ is the gate voltage above the threshold voltage V_T and t_{ox} is the thickness of the gate oxide. Eigenfunctions corresponding to the eigenvalues in Eq. (1) are given by

$$\psi(x,y,z) = \frac{1}{\sqrt{L_x L_y}} e^{j(k_x x + k_y y)} Z_i(z) \tag{5a}$$

$$Z_i(z) = \frac{1}{Ai'(-\xi_i) z_o^{1/2}} Ai\left(\frac{z}{z_o} - \xi_i\right) \tag{5b}$$

$$z_o = \frac{E_o}{qE_t} \tag{5c}$$

where $k_{x,y}$ are analog-type wave vectors in the x-y plane. The confined eigenfunctions $Z_i(z)$ describing the standing waves in the approximate triangular quantum well ($V(z) = qE_t z$) at the gate and the corresponding eigenstates are shown in Fig. 1 for the first two digitized energy levels.

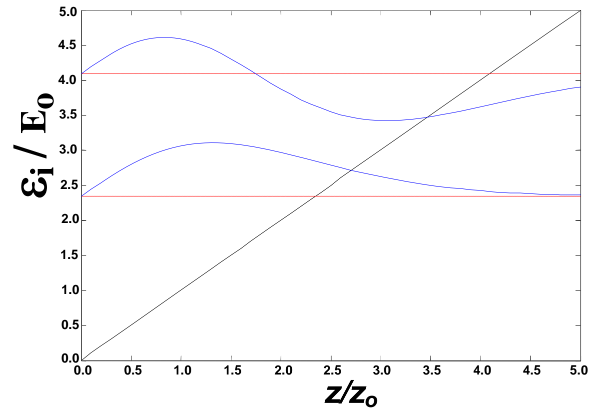

Fig. 1. Electron distribution in the first two quantized levels.

The average distance of the electron from the interface (z=0) for electrons [14] in the ground state is

$$z_{QM} = \frac{2}{3}\frac{E_o}{qE_t} \tag{6}$$

The electrons do not reside at the Si/SiO_2 interface as wavefunction vanishes there due to the quantum-confinement effect shown in Fig. 1. In the nano-MOSFET the gate oxide is a few nm (t_{ox} = 1.59 nm in our case). The distance z_{QM} of the electrons that is also a few nm cannot be neglected. Effective oxide thickness of the gate after correction for difference in permittivity of the SiO_2 and Si is given by:

$$t_{oxeff} = t_{ox} + \frac{\varepsilon_{ox}}{\varepsilon_{Si}} z_{QM} \approx t_{ox} + \frac{1}{3} z_{QM} \tag{7}$$

The gate capacitance C_G per unit area is smaller than C_{ox} and is given by

$$C_G = \frac{\varepsilon_{ox}}{t_{oxeff}} = \frac{C_{ox}}{1 + \frac{1}{3}\frac{z_{QM}}{t_{ox}}} \tag{8}$$

Fig. 2 shows the effective oxide thickness with the increase in the gate voltage as electrons are squeezed closer to the interface.

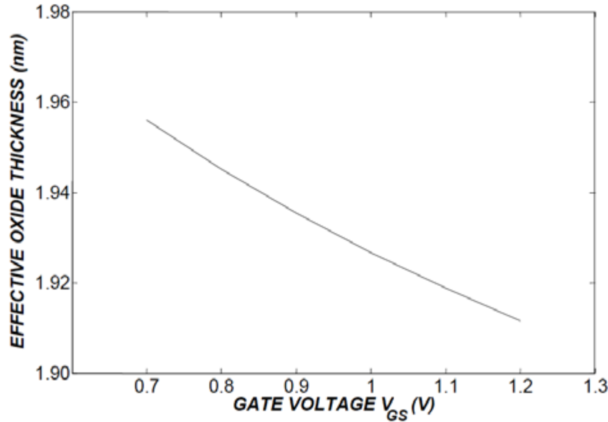

Fig. 2. Effective oxide thickness as a function of gate voltage with the quantum correction (t_{ox} = 1.59 nm).

Fairus and Arora [15] calculated the mobility for a QTD channel and found that the ratio $\mu_{\ell f} / \mu_b$ of the channel mobility to that in a bulk material is proportional to z_{QM} / λ_D where z_{QM} is the length of confinement and λ_D the de Broglie wavelength. Their results are in agreement with the data of Cooper and Nelson [16]. However, the data extracted from experiments by Tan and Ismail [17-18] follows an exponential trend ($\mu_{\ell f} = 0.0700\left(m^2/V.s\right)e^{-(V_{GS}/1.33)}$) as shown in Fig. 3.

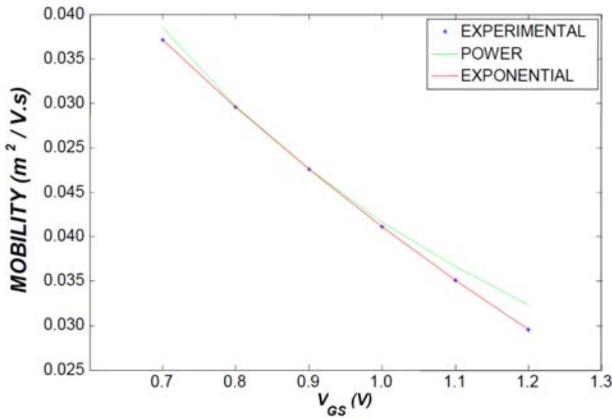

Fig. 3. Mobility as a function of gate voltage. The data (represented by *) is for the experimentally extracted mobility [7]. The dotted line is a plot of power law $\mu_{\ell f} = (V_{GS}/V_{QM})^{-2/3}$with V_{QM} = 6 mV and solid line that of exponential law with $\mu_{\ell f} = 0.0700\ m^2/V.s\ \exp(-V_{GS}/1.33\ V)$.

III. Low-Dimensional energy spectrum

In low-dimensional system as shown in figure 4, the energy spectrums of the respective system that consists of potential and kinetic energy is given by [8-9]

$$E_{kd} = E_{co} + \frac{1}{2}\left(\frac{P^2}{m^*}\right) = E_{co} + \frac{\hbar^2}{2m^*}\left[k_x^2 + k_y^2 + k_z^2\right] \tag{9}$$

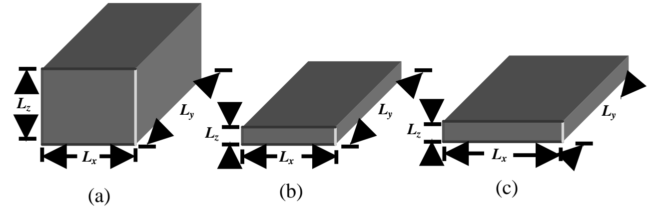

Fig. 4. Low-dimensional system for (a) quasi 3D (b) quasi 2D (c) quasi 1D

where P is the momentum, $k_{x,y,z}$ is the wave vector in three directions and d is the dimensionality of respective system.

For quasi 3 dimensional (Q3D) or bulk semiconductors as depicted in fig.4a, all the three Cartesian directions are much larger than the de Broglie wavelength ($L_{x,y,z} >> \lambda_D \cong 10nm$). Therefore the energy spectrum is analog-type in x, y and z-direction given by:

$$E_{k3} = E_{co} + \frac{\hbar^2}{2m^*}\left(k_x^2 + k_y^2 + k_z^2\right) \tag{10}$$

with the wavefunction, $\psi_{k3}(\vec{r})$

$$\psi_{k3}(x,y,z) = \frac{1}{\sqrt{\Omega}} e^{j(\vec{k}.\vec{r})} = \frac{1}{\sqrt{\Omega}} e^{j(k_x.x + k_y.y + k_z.z)} \tag{11}$$

This wave function describes the propagating waves in all three directions. In Q3D system the traveling wavelength in all 3 directions are traveling waves as shown in the wave function of equation (9). $k_{x,y,z}$ are the wave vector components with momentum $\vec{p} = \hbar\vec{k}$. E_{co} is the unaltered conduction band edge, m^* is the carrier effective mass assumed isotropic for all three dimensions and $\Omega = L_xL_yL_z$ is the volume of the

samples with $L_xL_yL_z$ is the length in each of the three Cartesian directions.

Figure 4b shows the Q2D of a nano-MOSFET system where the carriers are confined in the z-direction with L_z is much less than the de Broglie wavelength (λ_D) which is approximately 10nm. The other two dimensions, the x and y-dimensions are still in analogue characteristics with the length L_x and L_y are consider larger than de Broglie wavelength. The energy spectrum for Q2D system is given by

$$E_{k2} = E_c + \frac{\hbar^2 k_x^2}{2m_1^*} + \frac{\hbar^2 k_y^2}{2m_2^*} \tag{12}$$

with

$$E_c = E_{co} + \frac{\hbar^2}{2m_3^*}\left(\frac{\pi}{L_z}\right)^2 \tag{13}$$

and the wave function given by

$$\psi_{k2}(x,y,z) = \sqrt{\frac{2}{\Omega}} e^{j(k_x.x+k_y.y)} \sin\left(\frac{\pi z}{L_z}\right) \tag{14}$$

Equation (14) shows the wavefunction of a Q2D system where L_z is the effective length of confinement due to the penetration of the wavefunction in the classical forbidden region. In Q2D system, the wavelength in the z-direction becomes standing wave due to the quantum confinement effect (QCE) leaving the other two x and y-direction retains as traveling waves as shown in the wavefunction expression. $k_{x,y}$ are the wave vector components with momentum $\vec{p} = \hbar\vec{k}$ and E_c is the modified band edge that is lifted by the zero-point quantum energy due to QCE effects.

The wave-vector is digitized in the z-direction with the value $k_z = n\pi/L_z$ with only n=1 digit being considered in the quantum limit when most electrons occupy the lowest level of band edge. Due to QC effects in the z-direction of Q2D system the modified energy band diagram is expected as shown in figure 5. The energy band gap has been increased by the quantized band edge in z-dimensions for both conduction and valence band edge with either electron or hole carriers given by

$$\varepsilon_{oze(h)} = \frac{\pi^2\hbar^2}{2m_{e(h)}^* L_z^2} \tag{15}$$

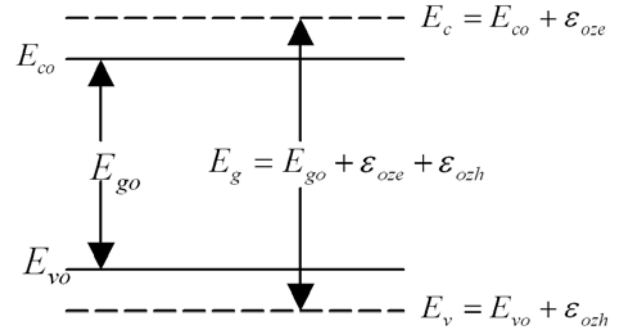

Fig. 5. The modified energy band diagram of Q2D system due to quantum confinement effect (QCE) in z-direction

For Q1D of a nanowire system only one dimension is larger than the de Broglie wavelength. The other two dimensions is quantum confined to the length less than de Broglie wavelength. This system is illustrated in figure 4c in which the length of L_z and L_y is confined. Thus, the energy spectrum of Q1D device is only analogue in the x-direction. The energy spectrum for nanowire with a rectangular cross-section is given by

$$E_{k1} = E_{c1} + \frac{\hbar^2 k_x^2}{2m_1^*} \tag{16}$$

with

$$E_{c1} = E_{co} + \frac{\pi^2\hbar^2}{2m_2^* L_y^2} + \frac{\pi^2\hbar^2}{2m_3^* L_z^2} \tag{17}$$

and the wave function given by

$$\psi_{k1}(x,y,z) = \sqrt{\frac{2}{\Omega}} e^{j(k_x.x)} \sin\left(\frac{\pi y}{L_y}\right)\sin\left(\frac{\pi z}{L_z}\right) \tag{18}$$

As depicted in equation (18), for Q1D system the quantum waves are standing wave in z and y-direction while in x-direction its remains as traveling waves. E_{c1} is the band edge in the quantum limit of a nanowire that is lifted from bulk conduction band edge E_{co} by the zero-point energy in the y and z-direction.

IV. LOW-DIMESIONAL CARRIER STATISTICS

The number of carriers available for conduction determines the electrical properties of the semiconductor devices. This number is found from the density of allowed states and the probability that these states are occupied. The probability that an available state with energy E is occupied by an electron under thermal equilibrium is given by the Fermi-Dirac probability density function ℑ(E) defined as

$$\Im(E) = \frac{1}{1+\exp\left(\frac{E-E_F}{k_B T}\right)} \tag{19}$$

where E_F is the fermi energy level defined as the energy level at which the probability of finding an electron, for $T > 0\ K$, is exactly one-half. E_F is purely mathematical parameter and provides a reference with which other energies can be compared. If $E = E_F$, $\Im(E) = ½$; means that the electron is equally likely to have an energy above fermi level as well as below it. If $\Im(E) = 1$ at $T = 0\ K$; means all energy levels below E_F are filled and all above it are empty. k_B is the Boltzmann's constant and T is semiconductor lattice temperature. If $E - E_F > k_B T$, the solution of equation (19) become much simpler since we can neglect the '1' and the function $\Im(E)$ can be approximated by the Boltzmann density function:

$$\Im(E) = \exp\left(\frac{E_F - E}{k_B T}\right) \tag{20}$$

The utilization of Boltzmann density function as given in equation (20), makes subsequent calculation much simpler and normally is justified in semiconductor device theory. However, Fermi-Dirac distribution function is necessary for certain properties of a very highly doped (degenerate) material. Due to recent advance devices was purportedly to be degenerately doped for the suppression of short channel effects (SCE), the exact solution of Fermi-Dirac distribution function is necessary. The solution is known as Fermi-Dirac Integral of order i and is given by:

$$\Im_i(\eta) = \frac{1}{\Gamma(i+1)}\int_0^\infty \frac{x^i}{e^{(x-\eta)}+1}dx \tag{21}$$

where

$$\eta = \frac{E_F - E_C}{k_B T} \tag{22}$$

and Γ is the gamma function that can be approximated by:

$$\Gamma(i+1) = i\Gamma(i) \tag{23}$$

The number of electrons per unit volume with energies between E and E+dE has been established to be $D(E)f(E)dE$, therefore the total carrier concentration in a band is obtain simply by integrating the Fermi-Dirac distribution function over energy band that is [19]:

$$n = \int_{E_C}^{E_{top}} D(E)f(E)dE \tag{24}$$

The carrier concentration (n_3 per unit volume for bulk, n_2 per unit area for 2D, and n_1 per unit length for 1D) as a function of normalized Fermi energy η_{Fd} ($d = 3, 2, 1$) with respect to the band edge is evaluated as

$$n_d = N_{cd}\Im_{\frac{(d-2)}{2}}(\eta_d) \tag{25}$$

Therefore, the electron concentrations for Q3D, Q2D and Q1D system are respectively given as

$$n_3 = N_{c3}\Im_{\frac{1}{2}}(\eta_3) \tag{26}$$

$$n_2 = N_{c2}\Im_0(\eta_2) \tag{27}$$

$$n_1 = N_{c1}\Im_{-\frac{1}{2}}(\eta_1) \tag{28}$$

with the effective density of states respectively defined as

$$N_{c3} = 2\left(\frac{m^* k_B T}{2\pi\hbar^2}\right)^{\frac{3}{2}} \tag{29}$$

DOI 10.5013/IJSSST.a.13.3B.07 ISSN: 1473-804x online, 1473-8031 print

$$N_{c2} = \frac{m^* k_B T}{\pi \hbar^2} \tag{30}$$

$$N_{c1} = \left(\frac{2m^* k_B T}{\pi \hbar^2}\right)^{1/2} \tag{31}$$

The complexity of solving Fermi-Dirac Integral is reduced if assumed the Boltzmann approximation and becomes (for non-degenerately doped devices)

$$\Im_i(\eta) = e^{\eta} \tag{32}$$

However, as the modern devices are mostly in the degenerately-doped sample, the exact solution of Fermi-Dirac integral is necessary and obtained as

$$\Im_i(\eta) = \frac{1}{\Gamma(i+1)} \frac{\eta^{i+1}}{i+1} \tag{33}$$

V. RESULTS AND DISCUSSION

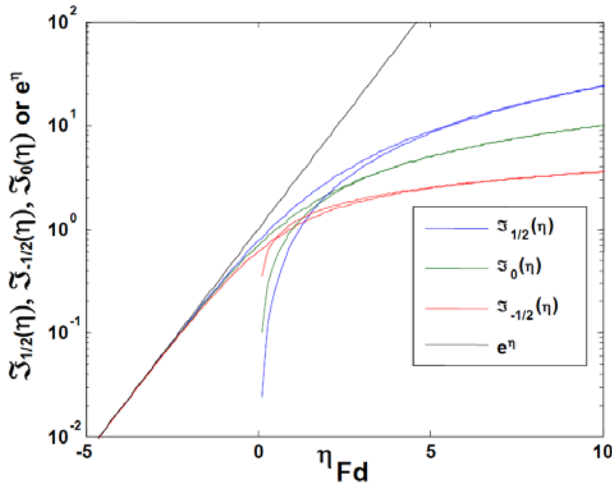

Fig. 6. The approximation of Fermi-Dirac integral as a function of Fermi energy η_{Fd} for non-degenerately and degenerately doped devices in $d = 3, 2$ and 1-dimensional system.

Figure 6 shows the plot of Fermi-Dirac integral of order one-half, zero and minus one-half against fermi energy (eta - η_{Fd}) for non-degenerately and degenerately doped samples with $d = 3, 2, 1$. In non-degenerately region in which η_{Fd} is small, the Fermi-Dirac integral is well approximated by equation (32) for all dimensions as indicates by the black color line. Similarly, in degenerately doped devices ($\eta_{Fd} > 0$), the blue, green and red color lines represent the very well estimated of Fermi-Dirac integral of equation (13) to its approximation in 3D (blue), 2D (green) and 1D (red) as can be derived from equations (25) respectively.

Figure 7 shows the normalized Fermi energy η_{Fd} as a function of normalized carrier concentration for d = 3, 2, 1. As expected in the non-degenerate (ND) regime $(E_F - E_c)_d$ as a function of $(n/N)_d$ is given by

$$(E_F - E_c)_d = k_B T \ln(n/N)_d \tag{33}$$

$(E_F - E_c)_d$ is a weak (logarithmic) function of carrier concentration, but varies linearly with temperature in the ND regime. However, for strongly degenerate statistics, the Fermi energy is independent of temperature and is a strong function of carrier concentration that can be given by:

$$(E_F - E_c)_d = \frac{\hbar^2}{m^*} 2\pi \left[\Gamma\left(\frac{d}{2}+1\right) n_d / 2\right]^{2/d} \tag{34}$$

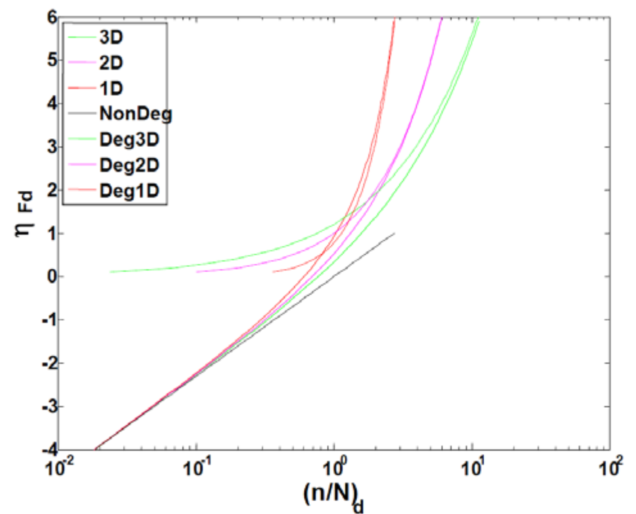

Fig. 7. The normalized Fermi energy as a function of carrier concentration. Approximation for non-degenerate regime and degenerate regimes are also shown.

The Fermi energy is proportional to $n_3^{2/3}$ for bulk (3D) configuration, n_2 for 2D nanostructure, and n_1^2 for 1D nanostructure. The 1D nanowires approach degeneracy at relatively lower values of carrier concentration as compared to 2D and 3D structures.

Induced and doped carrier density in most nanoscale devices are now in degenerate regime generating a great interest in degenerate statistics that is extensively used in the following section. Because of simplicity in the expressions for ND statistics, it is not uncommon to base the findings on ND statistics that sometimes leads to erroneous results.

VI. CONCLUSIONS

Based on the low-dimensional energy spectrum that invoked the effect of quantum confinement comparable to the De Broglie wavelength in the respective Cartesian directions of quasi 3D, 2D and 1D, the numerical analysis of nanostructure energy spectrum and carrier statistics was successfully done. For non-degenerately (ND) doped samples the Fermi-Dirac (FD) integral is well approximated by Boltzmann statistics for all dimensions. However, in degenerate doped quasi 3D, 2D and 1D device, the FD integral is found to be approximated by order one-half, zero and minus one-half respectively. The Fermi energy is revealed to be a weak (logarithmic) function of carrier concentration, but varies linearly with temperature in the ND regime. However, for strongly degenerate statistics, the Fermi energy is independent of temperature and is a strong function of carrier concentration. The Fermi energy is proportional to $n_3^{2/3}$ for bulk (3D) configuration, n_2 for 2D nanostructure, and n_1^2 for 1D nanostructure. In addition, the 1D nanowires approach degeneracy at relatively lower values of carrier concentration as compared to 2D and 3D structures.

ACKNOWLEDGEMENT

The authors would like to acknowledge the financial support from FRGS funds (FRG0248-TK-2/2010) and ERGS funds (ERGS0002-TK-1/2011) of Minister of Higher Education Malaysia (MOHE). The author is thankful to the Universiti Malaysia Sabah (UMS) for providing excellent research environment in which to complete this work.

REFERENCES

[1] International Technology Roadmap for Semiconductor (ITRS) – Emerging Research Devices vol.53, no.5, 2006.

[2] Sizov, D.S. et., al. "Influence of carrier statistics on InGaN/GaN device performance", IEEE International Conference of Semiconductor Electronics, 2004

[3] Arora V. K., "Quantum enginering of nanoelectronic devices: the role of quantum emission in limiting drift velocity and diffusion coefficient," Elsevier, Microelectronics Journal, vol. 31, no.11-12, pp 853-859. 2000

[4] Rahman A, Guo J, Datta S and Lundstrom M. "Theory of Ballistic Nanotransistors". IEEE Trans. Electron. Devices, Vol. 50, pp. 1853-1864, 2003.

[5] Natori K. "Ballistic metal-oxide-semiconductor field effect transistor". Journal of Applied Physics, 76 (8), pg 4879 - 4890, 1994

[6] Natori K. "Ballistic MOSFET Reproduces Current-Voltage Characteristics of an Experimental Device". IEEE Trans. On Electron Devices, Vol. 23, No. 11, pg 655-657, 2002

[7] Lundstrom M. "Elementary Scattering Theory of the Si MOSFET". IEEE Electron Device Letters, Vol. 18, No. 7, pages 361-363, 1997

[8] Ismail Saad, Michael L.p Tan, Ing Hui Hii, Razali Ismail And Vijay K. Arora. *Ballistic Mobility And Saturation Velocity In Low-dimensional Nanostructures*. Vol. 40, No. 3 (2009) pp 540-542. www.elsevier.com: Microelectronics Journal.

[9] Ismail Saad , Michael L. P. Tan, Aaron Chii Enn Lee, Razali Ismail And Vijay K. Arora. *Scattering-limited And Ballistic Transport In Nano-cmos Transistors*. Vol. 40, No. 3 (2009) pp 581-583. Www.elsevier.com: Microelectronics Journal.

[10] A. Rothwarf, "A New Quantum Mechanical Channel Mobility Model for Si MOSFET's," *IEEE Electron Device Letters*, vol. EDL-8, no. 10, pp. 499-502, 1987.

[11] Arora V.K. "Ballistic Quantum transport in Nano Devices and circuits". 2nd IEEE International Nanoelectronics Conference, 2008. INEC 2008. 24-27 March 2008 Page(s):573 – 578

[12] Michael L. P. Tan, Vijay K. Arora, Ismail Saad, Mohammad Taghi Ahmadi And Razali Ismail. *The Drain Velocity Overshoot In An 80 Nm Metal-oxide-semiconductor*. American Institute of Physics: Journal Of Applied Physics (2009).

[13] Frank Stern, "Self-Consistent Results for n-Type Si Inversion Layers," *Physical Review B*, vol. 5, pp. 4891-4899, 1972.

[14] Ismail Saad, Khairul A. M., Nurmin Bolong, Abu Bakar A.R and Vijay K. Arora, *Computational Analysis of Ballistic Saturation Velocity in Low-Dimensional Nano-MOSFET,* Int. Journal of Simulation, Sciences System and Technology (IJSSST), ISSN: 1473-804x online, 1473-8031 print, Vol.12. No. 3 (2011), pg1-6.

[15] A.M.T. Fairus and V. K. Arora, "Quantum engineering of nanoelectronic devices: the role of quantum confinement on mobility degradation," Elsevier, Microelectronics Journal, vol. 32, pp. 679-686, 2000

[16] J. F. Cooper and D. F. Nelson, "High-field drift velocity of electrons at the Si–SiO2 interface as determined by a time-of-flight technique," *Journal of Applied Physics,* vol. 54, no. 3, pp. 1445-1456, 1983.

[17] Michael L. P. Tan and Razali Ismail, "Modeling of Nanoscale MOSFET Performance in the Velocity Saturation Region," *Jurnal Elektrika*, vol. 9, no. 1, pp. 37-41, 2007.

[18] Michael Tan Loong Peng, Razali Ismail, Ravisangar Muniandy and Wong Vee Kin, "Velocity Saturation Dependence on Temperature, Substrate Doping Concentration and Longitudinal Electric Field in Nanoscale MOSFET," *Proceedings of the IEEE National Symposium on Microelectronics*, Kuching, Sarawak, Malaysia, pp. 210-214, December 2005.

[19] Ismail Saad , M. Taghi Ahmadi, Munawar A. R, Razali Ismail And Vijay K. Arora. *Numerical Analysis of Carrier Statistics In Low-dimensional Nanostructure Devices*. Penerbit UTM 2009: Jurnal Teknologi.